Dense Plasma Sources for Conventional and PI^3 Implanters

S. A. Nikiforov,
Efremov Research Institute of Electrophysical Apparatus (NIIEFA),
P. O. Box 42, Saint Petersburg, 189631, Russia
H. S. Lee, G. H. Kim, G. H. Rim,
Korea Electrotechnology Research Institute (KERI),
P. O. Box 20, Changwon, Korea 641-600

Abstract

Both conventional and PI^3 implanters require dense plasma sources for high productivity rate, and small sheath expansion in PI^3 besides. The problem of the creation of large volume uniform plasma in PI^3 facilities replaces that of beam forming in accelerators. Some aspects of ion extraction in both cases and Langmuir probe plasma diagnostics will be discussed. Plasma parameters of large volume multicusp dc hot cathode and inductively coupled RF plasma sources obtained with Langmuir probe and ion mass analyzer will be presented. Design features and performances of high current Freeman and ECR ion sources will be described.

1. Introduction

Thirty-three years divided the invention of ion implantation by accelerated ion beam in 1954 and plasma source ion implantation (PSII) in 1987. The former had been introduced into industry, mainly microelectronics and thus become conventional only after about 20 years of extensive researches, but the cost ineffectiveness slows down its wider applications. The latter allows to overcome some problems inherent to accelerator-based technology, such as limited average beam current, especially at low ion energies, line-of-sight nature, and complexity of the equipment. Anyway after a decade of the development the PSII technology, (or plasma immersion ion implantation: PI^3, plasma-based ion implantation: PBII), is still being hardly commercialized. Among a lot of scientific and technological problems to be solved the development of state-of-the-art dense plasma sources is one of key points for both accelerator-based and plasma-based ion implanters. In this paper we will discuss some aspects of ion extraction and plasma diagnostics with Langmuir probe and present results of R&D of various plasma sources.

2. Ion Extraction in Cylindrical Geometry

Ion extraction from a plasma in cylindrical geometry takes place in accelerators when ions are extracted through the slit in ion source and in PI^3 facilities when cylindrical target is to be treated. Extracted ion current is mainly dictated by plasma parameters (while transported beam current in accelerator is also by the extracting system structure of ion source). Langmuir probe theory of ion collection can be applied to obtain analytic expressions for the dependence of extracted current on different parameters and to estimate its value. Radial motion theory of Kagan and Perel [1] gives the following equation for the ion current onto a cylindrical probe immersed into non-isothermal plasma (T_i/T_e<<1):

$$I_{i_K} \cong 0.4 A_p e n_i \left(\frac{2kT_{e_{screen}}}{M_i} \right)^{1/2} \cdot \frac{r_s}{r_p}, \qquad (1)$$

where A_s is the probe area, n_i is the ion (plasma) density, M_i is the ion mass number, $T_{e\,screen}$ is the 'screening' electron temperature [2] ($T_{e\,screen} = T_e$ for Maxwellian EEDF), r_s is the sheath radius, and r_p is the probe radius.
It is applicable for the colissionless sheath if $n_i > n_{i\,min}$ defined by the condition:

$$\left(\frac{r_s}{\lambda_D}\right)^2 >> 19 \ , \tag{2}$$

where λ_D is the Debye length. At the upper limit of high density, and not too big bias voltage, $r_s/r_p \rightarrow 1$ and consequently Equation (1) gives Bohm current. The target radius is to be taken as a 'probe' one in case of PI^3. When ions are extracted from the plasma source through the slit, corresponding value is related with extracting system used and can be only roughly estimated.

The correlation between the sheath thickness and the value of extracting voltage for a given ion current is set by Child-Langmuir law. For cylindrical geometry it is:

$$I_i = \frac{2\sqrt{2}}{9}\left(\frac{e}{M_i}\right)^{1/2}\frac{l_p}{r_p}\frac{V^{3/2}}{\beta^2(r_s/r_p)} \ , \tag{3}$$

where V is the bias voltage and β^2 is the tabulated function [3]. Considering the product of β^2 and r_s/r_p the approximation is given by:

$$\left(\frac{r_s}{r_p}\right)\cdot\beta^2 \approx 0.35\left(\frac{r_s}{r_p}\right)^3 - 0.35 \ , \tag{4}$$

which is satisfactory for $20 > r_s/r_p > 2$ and then the ratio of r_s/r_p is given by:

$$\left(\frac{r_s}{r_p}\right)_{Ch} \approx \left[3.2\left(\frac{V}{T_{e\,screen}}\right)^{3/2}\frac{1}{\left(\frac{r_p}{\lambda_{D_e}}\right)^2} + 1\right]^{1/3} . \tag{5}$$

For $V >> T_e$ and big sheath enough we get from the expression (5):

$$r_{s_{Ch}} \propto n_i^{-1/3}\cdot T_e^{-1/6}\cdot V^{1/2}\cdot r_p^{1/3} \ , \tag{6}$$

and consequently for the ion current we have from Eq. (1):

$$I_i \propto n_i^{2/3}\cdot T_e^{1/3}\cdot M_i^{-1/2}\cdot V^{1/2}\cdot r_p^{1/3} \ . \tag{7}$$

The expression (7) shows relative influence of different parameters on the extracted current. It is complicated function of plasma parameters that implicitely depend on the chemical composition of working gas or vapor used in the plasma source. Thus such a simple trend like $I_i \propto M^{-1/2}$, that is often used when the performance of ion source is considered, may confuse rather than clarify the picture. Instead, such factors, as the value of the ionization potential of the element and either working substance atomic or molecular, should be considered. The performance of Freeman heavy ion source being discussed below in this paper is a good illustration to that. Meanwhile, inverse proportionality of the extracted current to the ion mass indicates the difference between the ion mass composition in a plasma and the extracted ion beam (accelerators) or flux (PI^3). The extracted current is defined mainly by the plasma density. The ion current increases with the extracting voltage approximately by its square root that is due to the increase of ion emitting area when the sheath extends. Practically, neither in ion accelerators nor in PI^3 facilities the stationary Child-Langmuir

sheath extend does realize. In the former the penetration of extracting field into the discharge chamber is limited by the extracting sleet (or hole) and in the latter short negative pulses are preferably used to stop the sheath at earlier phase.

In the PI³ models developed by Lieberman [4] and later by Scheuer *et al* [5] it is assumed that Child-Langmuir law is satisfied quasistatically during the sheath propagation. The equation for the sheath-edge position as a function of time in cylindrical geometry in normalized coordinates is [5]:

$$\frac{dR}{d\theta}=\frac{1}{R\beta^2(R)}\ , \qquad (8)$$

where $\theta \equiv \frac{4\sqrt{2}}{9}A^{3/2}\omega_{pi}t$; $R \equiv \frac{r}{r_t}$; $A \equiv \frac{eV}{kT_e}\cdot\frac{\lambda_D{}^2}{r_t{}^2}$.

The ion matrix sheath extent is approximated [5]:

$$R_0{}^2 \cong \left[(2A)^{1/2}+1\right]\cdot\left[(3A)^{1/3}+1/2\right];\ R_0 \equiv \frac{r_0}{r_t}\ , \qquad (9)$$

where ω_{pi} is the ion plasma frequency, r_t is the target radius, and r_o is the ion matrix sheath extent.

So, $$r_0 \propto n_i^{-5/12}\cdot V^{5/12}\cdot r_t^{1/6}\ . \qquad (10)$$

Substituting Eq. (4) into Eq. (8) we get:

$$\frac{dR}{d\theta}\approx\frac{1}{0.35(R^3-1)}\ . \qquad (11)$$

For the sheath extent big enough comparing with R_0 the expression (11) yields:

$$r_s \propto n_i^{-1/4}\cdot M_i^{-1/8}\cdot V^{3/8}\cdot r_t^{1/4}\cdot t^{1/4}\ . \qquad (12)$$

It is clear that the sheath extent weekly depends on the ion mass. Short pulse and dense plasma are required to overcome its relatively strong dependence on the bias voltage in order to limit the sheath thickness and thus to provide the high implantation efficiency in the batch process and conformal treatment of three-dimensional targets.

3. Plasma Diagnostics by Cylindrical Langmuir Probe

Different theories and methods of plasma diagnostics with single Langmuir probe (LP) are being used, often for the similar plasma parameters. We analyzed the applicability of basic models, describing the ion current onto single cylindrical LP, using Sonin plot. Sonin plot [6] represents the dependence of the normalized ion current I_i/I_s, measured at the probe potential eV_p = 15 kT_e , on the normalized probe radius and indicates the difference between the approaches clearly.

The normalized ion current onto cylindrical probe used is

$$I_{i_s}=\frac{1}{2\sqrt{\pi}}A_p e n_+\left(\frac{2kT_e}{M_i}\right)^{1/2}\ . \qquad (13)$$

Expressions given by different theories for the ion saturation current can be rewritten as follows:

Bohm [7]: $$I_{i_B}=0.4A_p e n_i\left(\frac{2kT_e}{M_i}\right)^{1/2}\ ; \qquad (14)$$

Kagan [1]: $I_{i_K} = 0.4 A_p e n_i \left(\frac{2kT_e}{M_i}\right)^{1/2} \cdot \frac{r_s}{r_p}$; (1)

OML [7]: $I_{i_{OML}} = \frac{1}{\pi} A_p e n_i \left(\frac{2kT_e}{M_i}\right)^{1/2} \cdot \left(\frac{V_p}{T_e}\right)^{1/2}$; (15)

So, for the normalized current we get:

$$\frac{I_B}{I_S} = 1.42; \quad \frac{I_K}{I_S} = 1.42 \cdot \frac{r_s}{r_p}; \quad \frac{I_{OML}}{I_S} = 1.13 \cdot \left(\frac{V_p}{T_e}\right)^{1/2} = 4.37;$$

Applying Eq. (5) of sheath-to-probe radius ratio we get:

$$\frac{I_K}{I_S} = 1.42 \frac{r_s}{r_p} \cong 1.42 \left[\frac{186}{(r_p/\lambda_D)^2} + 1\right]^{1/3}. \quad (16)$$

We carried out a series of experiments in multicusp hot cathode discharge using a cylindrical probe and proceeded the data using Kagan radial motion and OML formulas. The plasma density and operational pressure have been changed in wide range, providing collisionless sheath conditions. Figure 1 illustrates Sonin plot for the case of $T_i \to 0$ and represents the following data:

- Chen's numerical solution of ABR radial motion theory [8];
- Kagan radial motion theory (our approximation – Eq. (16));
- Laframboise simulation (stationary probe) [8];
- Alexeev simulation (non-stationary probe) [9];
- OML theory (low plasma density limit) [7];
- Bohm theory (high plasma density limit) [7];
- Our experimental results processed with both Kagan and OML formulas.

As it can be seen from Fig. 1 there is good agreement between Kagan, Laframboise and Alexeev results for "X" > 25, that corresponds to the plasma density of $n_e > 5.10^9$ cm^{-3} if $T_e = 1$ eV and the probe radius is 0.25 mm (as we used in experiment). They reach the high density limit of Bohm at the "X" ~ 2000, that corresponds to the plasma density of $n_e \sim 1.10^{12}$ cm^{-3} for $T_e = 1$ eV. Kagan's and Alexeev's results are close each other in wider range, up to X ~ 10, i.e. up to $n_e \sim 1.10^9$ cm^{-3} ($T_e = 1$ eV). The behavior of Kagan's and ABR' s theories is similar in all range because the same radial-motion approach is used. But ABR gives higher normalized current value.

The limits for Kagan and OML theories validity in Sonin plot scale:

Kagan: For $V_p/T_e=15$ $\frac{r_p}{\lambda_{D_e}} >> 0.74 \Rightarrow \frac{I_K}{I_S} << 1.42 \frac{r_s}{r_p} \cong 1.42 \left[\frac{186}{(r_p/\lambda_D)^2} + 1\right]^{1/3} \cong 9.8 \Rightarrow$ "X" >> 5

So, for $r_p = 0.25$ mm and $T_e = 1$ eV it gives $n_e >> 5.10^8$ cm^{-3}.

OML: According to Laframboise OML conditions are achieved when $\frac{r_p}{\lambda_{D_e}} < 1 \Rightarrow$ "X"< 5.

Acording to Alexeev OML can be applied only when $\frac{r_p}{\lambda_{D_e}} < 0.22 \Rightarrow$ "X"< 0.34.

Therefore, considering our experimental results, it is evident that the Kagan's approach can be used at least for all points except one that corresponds to the lowest density ("X"~5). This point is questionable because neither

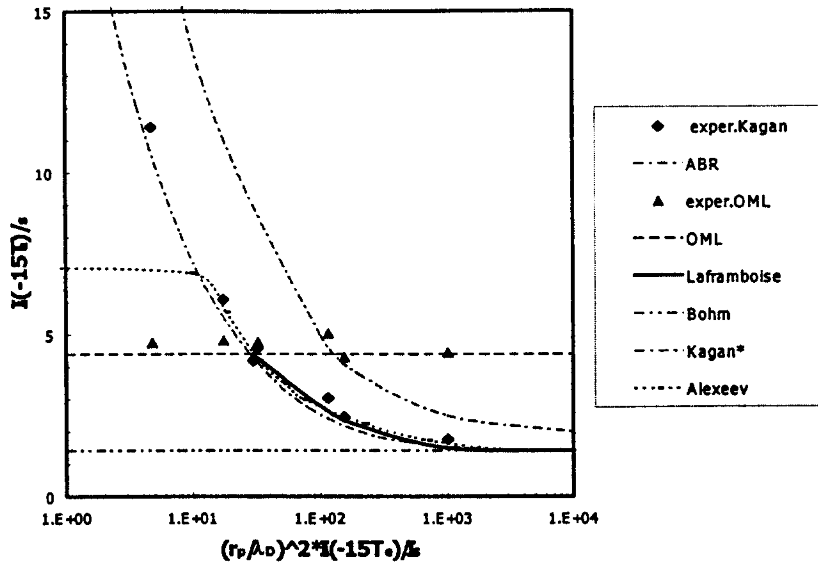

Fig. 1. Sonin plot for cylindrical probe. Comparision of different theoretical approaches and our experimental results processed applying Kagan and OML formulas.

Kagan's nor OML's approach is believed to be valid here. Kagan's procedure can be extended to lower plasma densities in two ways. First, by increasing the probe radius significantly (several times), that is may be unacceptable because of serious plasma disturbance. Another way is to use spherical probe. At the same radius it has the low-density limit of 15 time less than that for cylindrical probe. One more advantage of spherical probe is that it only can be used for the measurement of electron energy distribution function (EEDF) with Druyvesteyn procedure in anisotropic conditions.

We apply LP diagnostics for the investigation of plasma in hot cathode DC and inductively coupled RF discharges with cusp-geometry magnetic plasma confinement, which are being used in large-volume dense plasma sources for PI^3 facilities. Some results are being presented in the section 6.

4. Freeman Ion Source

The Freeman ion source [10] has been successfully used through decades and up to now is one of the most appropriate ion source for the generation of high-current heavy ion beams in conventional ion implanters [11, 12]. We developed the Freeman-type source designed as the metal-ceramic integral unit with 50 kV four-electrode accel/decel extracting system. Such a system allows to change the extracting voltage and the final beam energy independently. Thus, it optimizes the extracting voltage for different discharge parameters while it keeps the beam energy constant at the required value in the range of 5 ÷ 50 keV (single charged ions). Besides, it reduces high voltage breakdown probability in extracting gap. The source structure and layout view are shown in Fig. 2. The 2-mm-diameter tungsten cathode is fixed in molybdenum discharge chamber through boron nitride insulators. The magnetic field along the discharge chamber is produced by two sets of external permanent magnets mounted on the extracting electrode flange. Using of permanent magnets does not seriously effect on the source performance but significantly simplify its power supply system. Gases, liquids and solids can be used as a charge material. The discharge chamber has three inlets - the first is

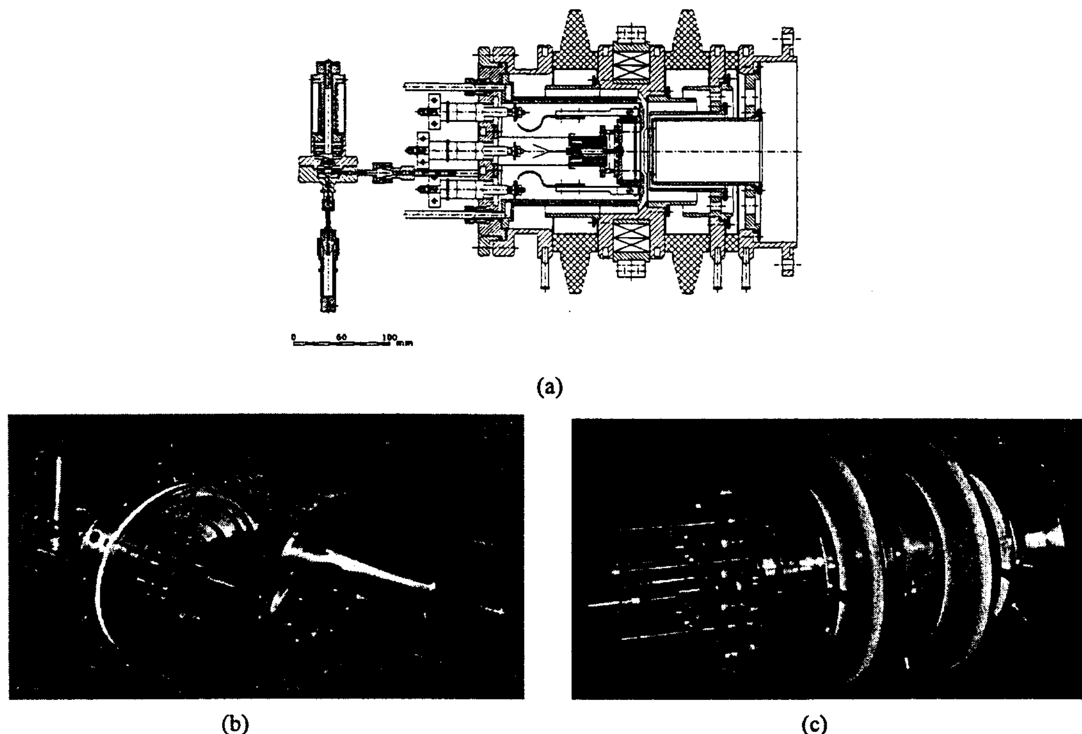

Figure 2. Freeman ion source.

(a) Cross section; (b) with removed shield electrode;

(c) assembled with 50 kV 4-electrode accel/decel system.

for a feed or support gas, the second is for a vapor delivered from outside container, and the third one is connected to the internal oven. The high-temperature all-metal flow controller with minimized through-pass volume has been developed for vapor flow control from outside container. It is supplied with heater and the operating temperature is adjusted in the range of 50 ÷ 400 °C. A set of changeable internal ovens with proper thermal shields is used to provide 400 ÷ 1100 °C temperature range. The discharge chamber with furnace is surrounded with water-cooled cylindrical electrode (see Fig. 2(b)) which has several functions. It serves as high voltage and heat removal shield, and protects the extracting ceramic insulator from coating with feed material, and prevents the outlet electrode of the source from radial alignment that may be caused due to the heating. There are no high voltage vacuum electrical feedthroughs in the source that makes its more reliable.

Ions are extracted through 40-mm × (0.5÷2.5)-mm slot. A different method from conventional one has been applied to compensate the deflection of the beam due to the magnetic field of ion source. Appropriate asymmetry of electrical field in the extraction gap is provided by different height of the profiled slot lips of the extracting electrode. The computer-simulated value of longitudinal displacement of lips was found to agree well with the experimental one. It is of order 0.2 mm and should be optimized for different ion species and extracting voltage. Several changeable extracting electrodes with different displacement are enough for all practical cases.

For 40 ÷ 50 keV beam energy and extracting slot 40 x 1.6 mm the beam current is 10 ÷ 20 mA when operating with different gaseous, liquid, and solid materials. The dependence of the transported beam current on the discharge current for some working substances is shown in Fig. 3. A Faraday cup with 40-mm-diameter input diaphragm was placed at 1 m from the source outlet slot. As it can be seen, 10 mA total transported ion beam current is provided for all

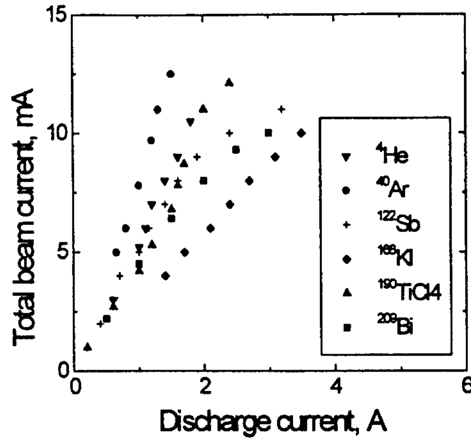

Figure 3. Transported ion beam current versus discharge current for different feed materials. Accelerating voltage is 50 kV.

materials presented with discharge current less than 4 A.

5. ECR Ion Source

Currently microwave ion sources are widely used in various accelerators and plasma facilities [10]. They can produce high-density large area plasma in the ECR or off-resonance mode. They also allow to operate with aggressive gases due to lack of hot cathode and provide the high atomic-to-molecule ion ratio in the extracted beam. We developed several versions of microwave sources for different applications [13]. ECR ion source intended for SIMOX implanters and intense neutron generators is shown in Fig. 4. The source has cylindrical stainless steel discharge chamber equipped with a three-layer dielectric window. A quartz disk provides vacuum sealing, a disk from alumina serves to reduce the reflection of microwave radiation and a disk from silicon nitride protects the window from the damage caused by secondary electrons accelerated in the extracting gap. After 700 hours of source operation the depth of craters formed in 12-mm-thick disk did not exceed 0.5 mm. There is movable diaphragm inside discharge chamber in front of the outlet electrode for tuning the standing wave ratio. Solenoid coils mounted on the cart produce a magnetic field along the source axis. The maximum of the plasma density is adjusted to be near the outlet electrode by changing of the coil current and moving them along the source axis as a whole. A 1 kW, 2.45 GHz microwave system comprises

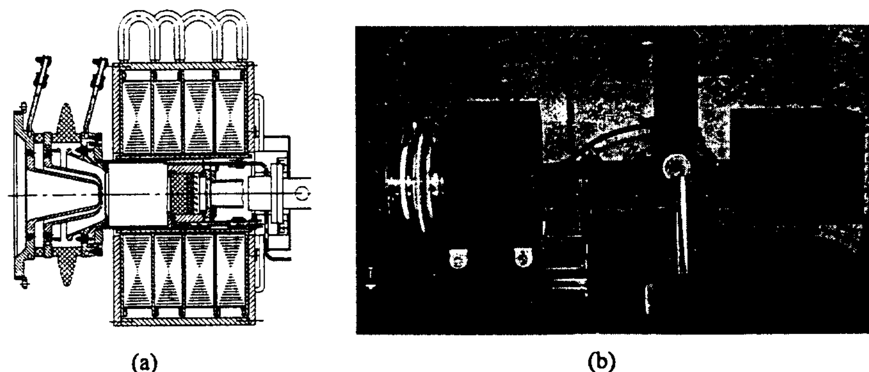

(a) (b)

Figure 4. ECR ion source.
(a) Cross section; (b) assembled with 1 kW, 2.45 GHz microwave system.

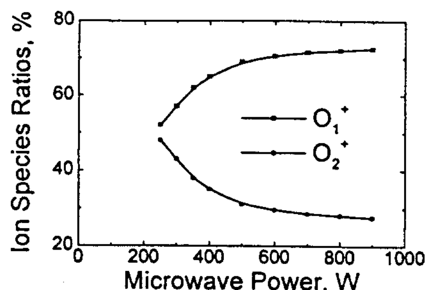

Fig. 5. Dependence of O^+_1 and O^+_2 ratio in extracted beam on microwave power.

circulator with dummy load and directional coupler. A 50 kV three-electrode multi-aperture accel/decel system is used for the ion extraction. Ions are extracted through one, four or seven holes 3 ÷ 6 mm in diameter, depending on a particular application. The upper part of extracting and suppressing electrodes is made of magnetic steel to reduce effect of crossed electric and magnetic fields on the beam divergence and high-voltage breakdown limit.

The dependence of atomic and molecular ion ratio in the oxygen beam on microwave power is shown in Fig. 5. Hereinafter the results mentioned were obtained using the outlet electrode with seven apertures of 3.5-mm diameter. The content of atomic component in the beam rapidly increases with the microwave power and reaches the value of 70% at the power of about 500 - 600 W. The beam current is 60 - 75 mA in this case and it increases even more sharply with the power. With further increasing of magnetron power, the growth is slowing down that is attributed to the reflection of microwave with increasing plasma density.

The source produces 70 mA oxygen ion beam with the maximum divergence of 20 - 30 mrad and 30 - 40 mm in diameter at the distance of half a meter without additional focusing. It was observed that the formation of the hydrogen ion beam differed essentially from that of oxygen or nitrogen ion beams. The divergence of the hydrogen beam is much higher that is due to strong influence of the magnetic field in the extraction area on light hydrogen ions.

6. Multicusp Hot Cathode and Inductively Coupled Plasma Sources

Kaufman and rf sources are widely used in beam-plasma apparatus and both are well adopted for large volume plasma generation in PI[3] implanters. As a preliminary step for a large-scale (120kV, 1000 liters) PI[3] facility we

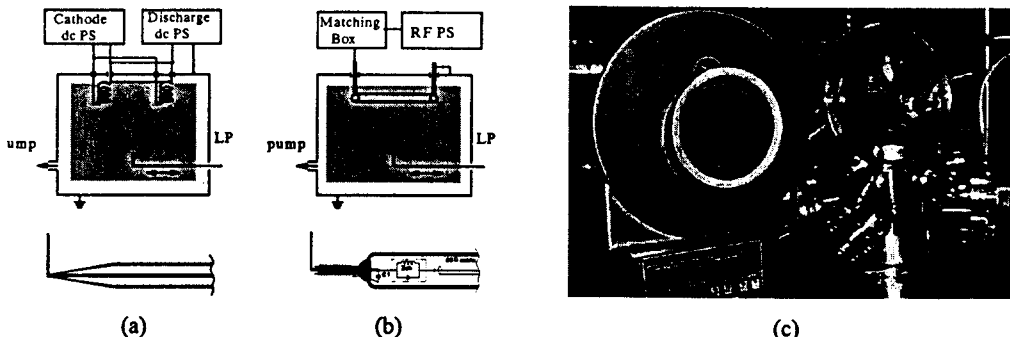

Fig. 6. Plasma sources for 30 kV, 18 liters experimental PI³D setup.

(a) and (b) – experimental arrangement and Langmuir probe for hot cathode and inductively coupled source respectively; (c) – layout view. Flange with immersed RF antenna for ICP is on the left, flange with 4 impregnated cathodes on processing chamber is on the right.

developed a 30 kV, 18-liter setup equipped with two changeable plasma sources based on dc hot cathode (HC) and 13.56 MHz inductively coupled (ICP) discharges. Multicusp magnetic arrangement is used to confine the plasma [14]. Two different top flanges were prepared to change the discharge type. The first one carries four impregnated cathodes, and the second one does immersed type two-half-ring rf antenna. The arrangement of electrodes in the processing chamber and its layout view are shown in Fig. 6.

The plasma parameters in the sources were compared as a function of the consumed power, operating pressure, and spatial position using a single Langmuir probe and ion mass analyzer. It was found that in HC discharge the plasma is more quiet and its density is higher when cathodes operate not in space charge limited mode (I) but in current saturation mode (II). Figure 7 illustrates this effect and also shows the difference in the population of high-energy tail of electron energy distribution function in both modes.

The dependence of the plasma density on the discharge power at different pressures for both kinds of sources is shown in Fig. 8. Cathodes heating power is taken into account. At 1 mtorr the plasma density of 10^{11} cm^{-3} is achieved for both sources. At higher pressure the HC discharge can produce the plasma with higher density up to 10^{12} cm^{-3}. The power transfer efficiency of ICP discharge decreases at high power while it increases at low power because of the capacitive-to-inductive mode jump. The measurements of radial distribution of the plasma density showed that it is quiet uniform and similar in both cases.

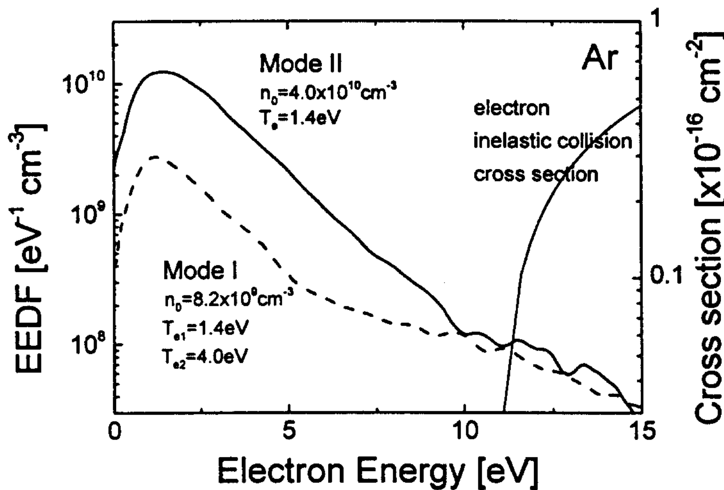

Fig. 7. Electron energy distribution function (EEDF) for two operational modes of hot cathode discharge.
In addition, electron inelastic collision cross section is plotted.
Gas – argon. P = 2mtorr, I_{disch} = 0.6 A, V_{disch} = 14 V (mode I), V_{disch} = 40 V (mode II).

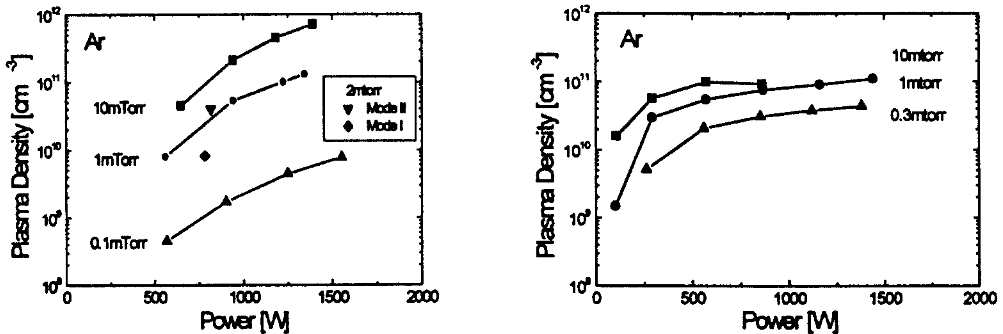

Fig. 8. Plasma density as a function of power. (a) - hot cathode source; (b) – ICP source.

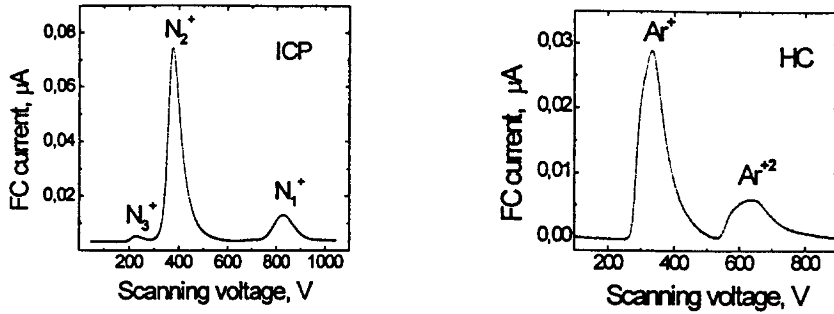

Fig. 9. Ion mass composition of extracted beam.
(a) – nitrogen, ICP source, P_{RF} = 300 W, P_{N2} = 1 mtorr; (b) – argon, hot cathode source, I_{disch} = 2 A, V_{disch} = 120 V (mode II), P_{Ar} = 2.2 mtorr (baratron).

It was found that nitrogen atomic-to-molecular ion ratio is weakly dependent on the pressure and the discharge power in both HC and ICP discharges and is of order 0.25 and 0.14, respectively. The content of N_3^+ is about 4% in ICP and is negligible in HC. In argon plasma the content of Ar^{2+} is negligible in ICP. The fraction of double charged ions is small in HC when the discharge voltage is kept at some tens of volts while it can amount to the value of 0.2 or more when the discharge voltage exceeds 100 V. Figure 9 shows examples of ion mass spectrums of nitrogen in ICP and argon in HC source.

A 120 kV, 10 kW, 1 m^3 plasma immersion ion implantation and deposition (PI^3D) facility has been designed as a further step in the development of PI^3D apparatus. It has horizontally mounted cylindrical processing chamber of stainless steel with the length of 1.5 m and the diameter of 1.0 m (Fig.10). Two kinds of plasma sources are being used – hot cathode dc and 13.56 MHz inductively coupled discharges. Six cathode units, where each unit comprises two thoriated-tungsten filaments, are distributed at the front door and rear flange of the chamber. Two-half-turn water-cooled RF antenna coated with Al_2O_3 is immersed into the chamber at its upper side. A set of Nd-Fe-B magnet bars is arranged around the chamber to confine the plasma. Two magnetrons or sputtering targets can be mounted onto the rectangular flanges placed along the chamber symmetrically to its axis for simultaneous or sequential deposition and implantation. The start-up of the facility operation is scheduled at the end of this year.

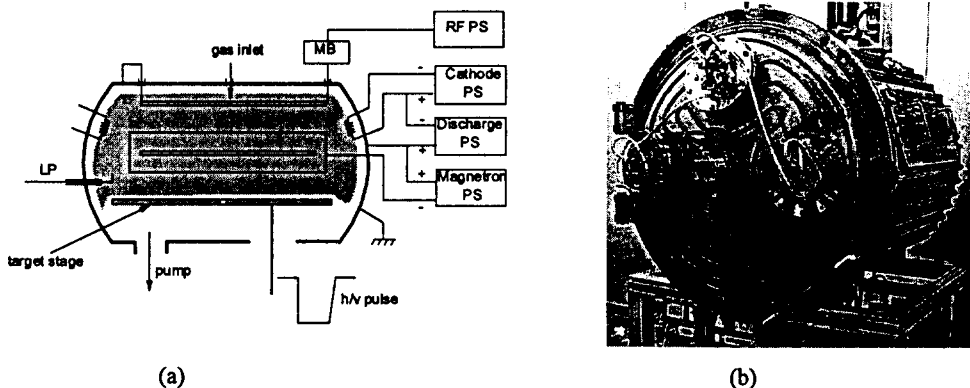

Fig. 10. 1m^3 processing chamber of 120 kV, 10 kW PI^3D facility, equipped with multicusp hot cathode dc and inductively coupled rf plasma sources. Two magnetrons or sputtering targets can be added for simultaneous or sequential implantation and deposition. (a) – structure; (b) – the chamber layout view.

7. Conclusion

A series of dense plasma sources has been developed for conventional and PI^3 implanters. The use of crossed electrical and magnetic field is exploited to enhance the source performance. Plasma parameters and ion extraction aspects have been investigated to optimize their design and operational conditions. Further researches should be carried out in this way to meet growing requirements of industry.

References

[1] Yu. M. Kagan and V. I. Perel, "Probe diagnostics of plasma", Usp. Fiz. Nauk. vol. 81, p.p. 409-452, 1963. {Sov. Phys. Usp. 6, 767 (1964)}.

[2] V. A. Godyak, R. B. Piejak and B. M. Alexandrovich, "Probe diagnostics of non-Maxwellian plasmas", J. Appl. Phys. vol. 73, no. 8, p.p. 3657-3663, 1993.

[3] I. Langmuir and H. Mott-Smitt, Gen. Electr. Rev. vol. 27, p.p. 449, 538, 616, 762, 810; 1924.

[4] M. A. Lieberman, "Model of plasma immersion ion implantation", J. Appl. Phys., vol. 66, no. 7, p.p. 2926-2929, 1989.

[5] J. T. Scheuer, M. Shamim, and J. R. Conrad, "Model of plasma source ion implantation in planar, cylindrical, and spherical geometries", J. Appl. Phys., vol. 67, no. 3, p.p. 1241-1245, 1990.

[6] P. M. Chung, L. Talbot and K. J. Touryan, Electric Probes in Stationary and Flowing Plasmas: Theory and Application, Berlin: Springer, 1975.

[7] L. Schott, "Electrical Probes", in Plasma Diagnostics, ed. W. Lochte-Holtgreven, Amsterdam: North-Holland, 1968.

[8] J. E. Allen, "Probe theories and applications: modern aspects", Plasma Sources Sci. Techmol. vol. 4, p.p. 234-241, 1995.

[9] B. V. Alexeev and V. A. Kotelnikov, Probe Method of Plasma Diagnostics, Moscow: ENERGOATOMIZDAT, 1988 /in Russian/.

[10] J. H. Freeman, et al "The production of heavy ion beams", A.E.R.E. Report R-8748, UK, 1977.

[11] The Physics and Technology of Ion Sources, Ed. by I. G. Brown, New York, J. Wiley & Sons.

[12] S. Nikiforov, V. Golubev, D. Solnyshkov, M. Svinin, G. Voronin, "Ion sources for use in research and applied high voltage accelerators", Proceed. of PAC95, Dallas, USA, vol. 2, p.p. 1004-1006, 1995.

[13] S. Nikiforov, D. Solnyshkov, G. Voronin, A. Solnyshkov,. "Development of an ECR ion source for accelerators and plasma processing applications" Proc. of EPAC94, London, UK, vol. 3, p.p. 1427-1429, 1994.

[14] S. A. Nikiforov, C. H. Cho, G. H. Kim, "30 kV experimental setup for plasma ion implantation and ion mixing", Proceed. of the 9th National Conf. on Application of Particle Accelerators in Medicine and Industry (Accelerators'98), St. Petersburg, Russia, the book of Abstracts, p.p.135-136, 1998.